Asymptotic analysis in time-dependent calculations with divergent coupling

A. Keller
Laboratoire de Photophysique Moléculaire du CNRS, Bâtiment 213, Université Paris Sud, Campus d'Orsay, 91405 Orsay, France
(Received 24 October 1994; revised manuscript received 16 February 1995)

An efficient time-dependent method is presented to obtain, at any time, the nuclear wave functions corresponding to the intense field photodissociation of homonuclear ions, which possess a divergent electronic transition moment, as the internuclear separation increases. It consists of splitting the wave functions into two parts, one part corresponding to the internal region and the second to the asymptotic part. The propagation of the wave packet's asymptotic part is done analytically even during the field interaction. The advantage of the method presented here is that the extension of the grid, needed to represent the wave packets, is fixed once and for all. Therefore, the numerical effort is reduced to the propagation in a previously fixed region of space, regardless of the duration of the field. The method is applied to calculate the proton kinetic energy spectrum in the photodissociation of the H_2^+ molecule.

PACS number(s): 42.50.Hz, 33.80.Gj, 34.50.Rk, 33.80.Wz

I. INTRODUCTION

Since the advent of intense lasers, many studies have been devoted to the photodissociation dynamic of molecules in the presence of a laser field, with strength comparable to the internuclear binding energy. This high intensity regime is obtained by concentrating the laser energy in very short pulses, which implies a time-dependent theoretical approach. In most of the studies (except in Ref. [1]), this approach consists of solving numerically the Schrödinger equation by sampling the initial nuclear wave function on a grid and then numerically propagating it on the radiatively coupled electronic potential energy surfaces until the photodissociation process ends. Several measurable quantities may then be calculated to get insight into the dynamic of the molecule subjected to intense field. From the point of view of numerical calculation, these observables can be classified into two groups.

The first group consists of quantities which can be obtained without knowing the behavior of the wave packet at large internuclear separation (asymptotic part of the wave packet). The final vibrational state of the molecule (which can be calculated by projection of the wave packet on the vibrational states of the free molecule) and the total photodissociation probability (which may be calculated by time integrating the density current vector flux, at a not too large internuclear separation) are such measurable quantities. Because they can be performed ignoring the behavior of the wave packet at large distance, these calculations can be done with small grid extension, absorbing (with an optical potential, for instance) the wave packet on the edge of the grid, and therefore are not very time consuming.

A second type of observable, on the contrary, requires for calculation the full wave packet (including very large internuclear separation) at the end of the photodissociation process. We call these quantities asymptotic observables. They correspond in general to detailed information about fragment properties. From now on, we will focus on this second type of observable and more precisely on the fragment kinetic energy spectrum which is typically that of such an asymptotic observable.

Several methods have been proposed to calculate such detailed properties of fragments. These methods were first developed in the context of time-dependent collision and half-collision studies. The aim of these methods was to obtain the scattering S matrix by wave packet propagation. Spatial Fourier transform of the wave packet and time Fourier transform of correlation type function [2–4] methods have been developed. These procedures are based on the fact that, in general, the intermolecular forces have a finite space extension, implying thus the existence of an asymptotic region of space where the fragments behave like free particles. The same procedures have been applied to photodissociation processes (see, for instance, Ref. [5]) in the case where the radiative interaction (i.e., the permanent or induced dipole moment) has a finite space extension. In this case, Heather and Metiu [6] have developed a very efficient scheme which takes advantage of the existence of an outer region free of forces. Their method consists of splitting the wave packet into an interaction part, subject to molecular and field forces, and an asymptotic part, where propagation is done analytically by considering it as a free wave packet.

It is well known that homonuclear ions with an odd charge possess a pair of so-called charge resonant electronic states [7,8]. The transition dipole moment between these states has the peculiar property of diverging linearly as the internuclear distance increases. It has been suggested [9] that because of this strong coupling these molecules may be good candidates for studies of nonlinear effects.

Because of this electronic asymptotic coupling, the before mentioned method cannot be directly applied during the laser interaction. This problem has recently been addressed in the time-independent Floquet scattering framework [10,11,1].

Until now, in the context of time-dependent methods, the techniques used to calculate the kinetic energy spectrum for this type of molecules consisted of propagating the full wave packet, on a very large grid, during the whole field duration, and then in analyzing it, only after the radiative interaction has ended, in order to extract free fragment properties. This analysis may consist of a spatial Fourier transform of the wave packets [12,6] or of projecting the wave packets on previously calculated eigenfunctions, corresponding to the continuum part of the Hamiltonian [13], and also of calculating an energy resolved flux [14]. These procedures are very time consuming due to the grid extension required to describe the full wave packets during the field interaction. Furthermore, when the pulse length increases, the computation time increases not only because the final time propagation is larger but also because the grid needed to represent the spreading and displacement of wave packets during this additional amount of time also increases.

The aim of this paper is to show a propagation method which allows the description of the entire wave packet while using a restricted grid. The method is an adaptation of the Heather and Metiu scheme [6], which consists of splitting the wave function into two parts, one corresponding to the internal region and the second one corresponding to the asymptotic part. The propagation of the wave packet's asymptotic part is done analytically even during the field interaction. Because of the divergent coupling, the asymptotic wave packets cannot be considered (as in Ref. [6]) as a superposition of independently propagating plane waves. Nonetheless, it will be shown that the propagation can be done in the spirit of Ref. [6], if the wave packet is taken as a superposition of Volkov waves in the asymptotic region of space.

The advantage of the method presented here is that the extension of the grid is fixed once and for all, regardless of the duration of the pulse. The principle of the propagation method, emphasizing the propagation of the wave packet's asymptotic part, will be presented in Sec. II.

The method will be applied to the photodissociation of $H_2{}^+$ by intense laser pulses ($I = 10^{13}$ to 10^{14} W/cm^2) with a wavelength $\lambda = 330$ nm. It is well established that for such a wavelength and intensities the photodissociation of $H_2{}^+$ exhibits above threshold dissociation (ATD). This process has been invoked to explain the appearance of successive peaks, separated by the energy of one photon (in the body-fixed frame), in the proton kinetic energy spectrum [15,16]. The possibility of continuum-continuum absorption and stimulated emission, during the dissociation of the molecule, has been the subject of many theoretical studies [17–19]. In Sec. III the kinetic energy spectrum is calculated with the present method. For testing purposes it will be compared with the Heather and Metiu method [6] and for several laser intensities with published results [19].

II. THEORY

For the molecule being described within the Born-Oppenheimer approximation, we assume that only the two charge resonant electronic states ($^2\Sigma_g, ^2\Sigma_u$) are coupled by the laser field $E(t)$. The equations describing the nuclear motion of the diatomic molecule interacting with the laser pulse are

$$i\hbar\frac{\partial\psi_1(R,t)}{\partial t} = -\frac{\hbar^2}{2\mu}\frac{\partial^2\psi_1(R,t)}{\partial R^2} + V_1(R)\psi_1(R,t) - \mu_{12}(R)E(t)\psi_2(R,t) \ , \tag{1a}$$

$$i\hbar\frac{\partial\psi_2(R,t)}{\partial t} = -\frac{\hbar^2}{2\mu}\frac{\partial^2\psi_2(R,t)}{\partial R^2} + V_2(R)\psi_2(R,t) - \mu_{12}(R)E(t)\psi_1(R,t) \ , \tag{1b}$$

where $\psi_1(R,t)$ [$\psi_2(R,t)$] is the wave function describing the nuclear motion of the molecule in the ground (excited) electronic state, $V_1(R)$ [$V_2(R)$] is the ground (excited) state potential energy curve, $\mu_{12}(R)$ is the transition dipole moment, and μ is the reduced mass of the system. The rotational motion will not be considered in this paper.

A. Splitting of space

Following Ref. [6], one can divide the space into two regions, an asymptotic region (A) where the potential energies $V_j(R)$ ($j = 1, 2$) are zero and an interaction region (I) where interaction potential acts. The wave functions are in turn split as follows:

$$\psi_j(R,t) = \psi_j^I(R,t) + \psi_j^A(R,t) \quad (j = 1,2) \ ,$$

where $\psi_j^I(R,t)$ is nonzero in the interaction region and $\psi_j^A(R,t)$ is nonzero in the asymptotic region. This is done through some smooth function $f(R)$ which is essentially equal to 1 in the interaction region and equal to 0 in the asymptotic one, such that

$$\psi_j^I(R,t) = f(R)\psi_j(R,t) \ , \tag{2a}$$

$$\psi_j^A(R,t) = [1 - f(R)]\psi_j(R,t) \ . \tag{2b}$$

B. Analytical propagation of $\psi_j^A(R,t)$

The linearity of the Schrödinger equation allows us to propagate separately $\psi_j^I(R,t)$ and $\psi_j^A(R,t)$. The aim of this section is to show that we can propagate $\psi_j^A(R,t)$ analytically and therefore limit the numerical effort to computing $\psi_j(R,t)$ only on a previously fixed region of space. Actually, in the asymptotic region the potential energy is zero and the transition dipole moment between the two charge resonant states of the homonuclear ion diverges as $\frac{eR}{2}$ (e being the electric charge of the electron). The coupled equations describing the evolution of the asymptotic wave function $\psi_j^A(R,t)$ are then

$$i\hbar\frac{\partial\psi_1^A(R,t)}{\partial t} = -\frac{\hbar^2}{2\mu}\frac{\partial^2\psi_1^A(R,t)}{\partial R^2} - \frac{eE(t)R}{2}\psi_2^A(R,t) \ , \tag{3a}$$

$$i\hbar\frac{\partial\psi_2^A(R,t)}{\partial t} = -\frac{\hbar^2}{2\mu}\frac{\partial^2\psi_2^A(R,t)}{\partial R^2} - \frac{eE(t)R}{2}\psi_1^A(R,t) \ . \tag{3b}$$

These coupled equations (3) can be decoupled, introducing the following new wave functions:

$$\chi_1(R,t) = \frac{1}{\sqrt{2}}[\psi_1^A(R,t) + \psi_2^A(R,t)] \ , \tag{4a}$$

$$\chi_2(R,t) = \frac{1}{\sqrt{2}}[\psi_1^A(R,t) - \psi_2^A(R,t)] \ . \tag{4b}$$

The time evolution of these new functions is determined by the following equations:

$$i\hbar\frac{\partial\chi_1(R,t)}{\partial t} = -\frac{\hbar^2}{2\mu}\frac{\partial^2\chi_1(R,t)}{\partial R^2} - \frac{eE(t)R}{2}\chi_1(R,t) \ , \tag{5a}$$

$$i\hbar\frac{\partial\chi_2(R,t)}{\partial t} = -\frac{\hbar^2}{2\mu}\frac{\partial^2\chi_2(R,t)}{\partial R^2} + \frac{eE(t)R}{2}\chi_2(R,t) \ . \tag{5b}$$

As the two equations (5) are the same, except for the sign change in the field term, we restrict the following discussion to Eq. (5a). To obtain the results for the second equation, we just have to change the electric field $E(t)$ by $-E(t)$ in the first one.

The equation giving the time evolution of $\chi_1(R,t)$, Eq. (5a), is formally analogous to the equation describing the motion of a free electron in an electric field $E(t)$ (where R is now to be interpreted as an electronic coordinate). It is well known [20,21] that the Volkov states are solutions of this equation. Let $u_k(R,t,t_i)$ be the time-dependent Volkov states which reduce to a plane wave at time t_i:

$$u_k(R,t,t_i) = \exp\{i[k+\Delta(t,t_i)]R\} \times \exp\left[-i\int_{t_i}^{t} dt' \frac{\hbar}{2\mu}[k+\Delta(t,t')]^2\right] \ , \tag{6}$$

where

$$\Delta(t,t_i) = \frac{e}{2\hbar}\int_{t_i}^{t} dt' E(t') \ . \tag{7}$$

The set of functions $\{u_k(R,t,t_i)\,; k \in]-\infty,+\infty[\}$ may be used as a basis set for expanding the wave functions at any time $t \geq t_i$. This is the analog of expanding the wave packet in terms of plane waves, describing the translational motion of field free fragments, when no coupling is present in the asymptotic region [6]. If we know the expansion coefficients $\hat{\chi}_1(k,t_i)$ such that the expression of $\chi_1(R,t_i)$ at time t_i is

$$\chi_1(R,t_i) = \int dk\, \hat{\chi}_1(k,t_i) u_k(R,t_i,t_i) \ , \tag{8}$$

which reduces to the Fourier transform

$$\hat{\chi}_1(k,t_i) = \frac{1}{2\pi}\int dR\, \chi_1(R,t_i) e^{-ikR} \ , \tag{9}$$

then the later evolution of $\chi_1(R,t)$ $(t \geq t_i)$ is simply determined by the time evolution of the basis set $\{u_k(R,t,t_i)\}$:

$$\chi_1(R,t) = \int dk\, \hat{\chi}_1(k,t_i) u_k(R,t,t_i) \ . \tag{10}$$

Another way of showing this is to look for the time evolution in momentum space, thus defining the Fourier transform of $\chi_1(R,t)$ at time t:

$$\hat{\chi}_1(k,t) = \frac{1}{2\pi}\int dR\, \chi_1(R,t) e^{-ikR} \ . \tag{11}$$

Using Eq. (10) and the definition of the $u_k(R,t,t_i)$ Eq. (6) we obtain

$$\hat{\chi}_1(k,t) = \hat{\chi}_1(k-\Delta(t,t_i),t_i) \times \exp\left[-i\frac{\hbar}{2\mu}\int_{t_i}^{t} dt'\,[k-\Delta(t,t')]^2\right] \ . \tag{12}$$

Therefore the time evolution of $\hat{\chi}_2(k,t)$ which is defined as $\hat{\chi}_1(k,t)$ in Eq. (11) is given by

$$\hat{\chi}_2(k,t) = \hat{\chi}_2(k+\Delta(t,t_i),t_i) \times \exp\left[-i\frac{\hbar}{2\mu}\int_{t_i}^{t} dt'\,[k+\Delta(t,t')]^2\right] \ . \tag{13}$$

We see that the time evolution of the $\hat{\chi}_j(k,t)$ $(j = 1,2)$ functions (i.e., in momentum space) is very simple. To obtain $\hat{\chi}_j(k,t)$ at any time $t \geq t_i$, we just have to shift in k space the initial $\hat{\chi}_j(k,t_i)$ by the laser pulse area $\Delta(t,t_i)$ and to multiply by a phase factor. The asymptotic momentum wave functions can be recovered using Eq. (4).

C. Propagation algorithm

The wave packet propagation algorithm is divided into the following steps.

(i) Define the initial wave function $\psi_j(R,t=0)$ $(j = 1,2)$, sampled on a grid extending from 0 to $R_{\max}$.

(ii) Propagate numerically (with the split operator method, for instance) the two coupled wave packets until their values at the end of the grid reach a fixed value ϵ [i.e., until $|\psi_j(R_{\max},t)|^2 > \epsilon$ $(j = 1\ or\ 2)$]. The time at which this condition is satisfied defines the time t_i of Eqs. (12) and (13).

(iii) Split the wave packets [Eq. (2)] using $f(R)$.

(iv) Propagate analytically the asymptotic part of the wave packets from t_i to t [Eqs. (12) and (13)].

(v) Go to the first step with the interaction part of the wave packets as initial wave functions.

During the propagation, the pulse area $\Delta(t,t')$ has to be calculated as well as its integral. Every time step (iv) is reached the propagated asymptotic part of the wave packet is added to the previous ones. At the end of the propagation we can reconstruct the full wave packets, adding the remaining interaction part $\psi_j^I(R,t)$ to the coherent sum of the asymptotic parts. Contrary to the propagation methods consisting of a full description of the wave packets on the grid, we see that here, regard-

less of the length of the pulse, the extension of the grid and therefore the number of points required to represent the wave function at a given resolution is fixed once and for all.

III. NUMERICAL RESULTS

The theory presented in the preceding section will be applied to the multiphoton photodissociation of the $H_2{}^+$ molecule. It is well established that the photodissociation of $H_2{}^+$ exhibits above threshold dissociation (ATD). This process has been invoked to explain the proton kinetic energy spectra obtained experimentally. These spectra are typically asymptotic observables, as discussed in Sec. I, and constitute a good test of our method. The calculation of the photodissociation probability distribution as a function of the proton kinetic energy will be the subject of the first part of this section. In the second part we will compare our method to the propagation method of Ref. [6] and with the results of Ref. [19].

A. Proton kinetic energy spectrum calculation

The fragment wave vector probability distribution is given by

$$P(k)dk = \lim_{t\to\infty}[|\hat{\psi}_1^A(k,t)|^2 + |\hat{\psi}_2^A(k,t)|^2]dk \ . \qquad (14)$$

The $\hat{}$ symbol denotes Fourier transform:

$$\hat{\psi}_j^A(k,t) = \frac{1}{2\pi}\int dR\, \psi_j^A(R,t)e^{-ikR} \qquad (15)$$

and $\lim_{t\to\infty}$ means that t is such that the laser electric field is off and the remaining interaction part of the wave packet is a superposition of bound states only. We have seen in Sec. II that asymptotical part propagation is done in momentum space [Eqs. (12) and (13)], therefore at the end of the propagation we obtain directly the needed $\hat{\psi}_j^A(k, t\to\infty)$ wave functions in k space. The fragment kinetic energy spectrum is then given by

$$\mathcal{S}(E)dE = \frac{1}{\hbar}\sqrt{\frac{\mu}{2E}}P\left(\frac{1}{\hbar}\sqrt{2\mu E}\right) \ . \qquad (16)$$

The total photodissociation probability may be obtained by summing $P(k)$ over k:

$$P_d = \int dk\, P(k) \ . \qquad (17)$$

The conservation of the wave packet norm provides another way to obtain P_d:

$$P_d = \lim_{t\to\infty}\left(1 - \int dR\, |\psi_1^I(R,t)|^2\right) \ . \qquad (18)$$

B. Computational features

The numerical wave packet propagation is performed using the three term split operator in conjunction with fast Fourier transform (FFT) [22,23] and approximating the exponential of the operators by the Cayley formula [24]. Time integration of highly oscillating terms, such as $\Delta(t,t')$, are conducted by the so-called Filon technique [25].

Wave functions are sampled on a grid of $N_R = 512$ points extending to $R_{\max} = 15$ Å. The highest kinetic energies that can be reached with this sampling ($\Delta R = 3\times10^{-2}$ Å) are greater than 3×10^5 cm^{-1}. The time step is taken as $\Delta t = 0.02$ fs, which allows for a good description of the oscillating field (50 points per period for a 330 nm wavelength). A larger time step might be taken by using a recently developed split operator method involving more than three exponentials [18,26]. Every time the splitting procedure is applied, a Fourier transform is performed on the asymptotic wave packets [steps (iii) and (iv) of the propagation algorithm] to apply Eqs. (12) and (13) in momentum space. As suggested by the authors of Ref. [6], to increase the momentum resolution Δk, the wave packets in momentum space are represented in a larger grid with $N_k = 2048$ points and with the same resolution ΔR. We will see that the asymptotic propagation is applied very few times, then increasing the number of points does not affect the efficiency of the algorithm. At the end of the propagation, it is checked that Eqs. (17) and (18), for the total photodissociation probability, give the same result. The value of ϵ in step (ii) is taken as 10^{-10}.

The splitting function Eq. (2) is taken as [6]

$$f(R) = \left(1 + \exp\left[\frac{R-R_0}{\sigma}\right]\right)^{-1} \ , \qquad (19)$$

where R_0 represents the point dividing the interaction and the asymptotic region and σ controls the extension of the transition zone between these two regions. In our calculations we choose $R_0 = 11$ Å, such that for $R > R_0$ the wave packet cannot return to the interaction region, which is an implicit requirement of the algorithm. This can be tested at the end of the calculation by verifying that the asymptotic wave packets do not contain negative momentum components [i.e., $\hat{\psi}_j^A(k, t\to\infty) = 0$ for $k < 0$].

A compromise has to be made to assign a value for the σ parameter. Indeed, if we want to sharply split up the internal from the asymptotic region we must choose a very small value for σ, but if this value is too small then the variation of the $f(R)$ function will be too sharp, introducing high momentum components and thus accelerating temporarily the wave packets. Of course, such an artifact does not modify the result of calculation but increases the number of splitting operations required. A good compromise is obtained with $\sigma = 0.1$ Å.

A Gaussian shape for the laser electric field is taken:

$$E(t) = E_0 \exp\left[-\left(\frac{t-4\tau}{\tau}\right)^2\right]\cos(w_L t). \qquad (20)$$

The Born-Oppenheimer potential energy curves corresponding to the $^2\Sigma_g$, $^2\Sigma_u$ electronic states of $H_2{}^+$ are taken from Ref. [27] and the transition dipole moment

from Ref. [28] which have the correct asymptotic behavior.

C. Tests of the method

As a first test, we compare the present method with the method of Ref. [6], where the asymptotic part of the wave packet is propagated as a free wave packet. In other words, the wave packet is expanded in terms of plane waves instead of Volkov waves (which corresponds to setting $\Delta = 0$ in the algorithm presented here). Because this method assumes that no force acts within the asymptotic region, it must be applied only after the field interaction ends. Actually, during the laser pulse, due to the divergent coupling, no force free region exists. Thus the full wave packet has to be numerically propagated during the whole duration of the field interaction.

For a very short laser pulse the two methods lead to almost the same results. Actually, if during the laser interaction the wave packet has no time to reach the end of the grid, then the splitting of the wave packet will be done only after the laser pulse is switched off, even in the present method. Table I shows the photodissociation probabilities for such a very short pulse ($\tau = 5$ fs and $I = 8.75 \times 10^{13}$ W/cm^2), and the kinetic energy spectra calculated with both methods are presented in Fig. 1. The same R-grid and time sampling parameters have been used for the two methods, resulting in the same CPU time. A very good agreement is obtained for such a very short laser pulse.

For a longer laser pulse ($\tau = 20$ fs), a larger R grid must be taken to use the method of Ref. [6]. Indeed, during these 20 fs the grid needed to represent the full wave packet is very large ($R_{\max} = 120$ Å), thus requiring $N_R = 4096$ points so that the sampling rate is the same as in the present method.

The kinetic energy spectra calculated with the two methods are presented in Fig. 2 and the branching ratios for one-, two-, and three-photon transitions, as well as the total photodissociation probability calculated with the two equations (17) and (18) are presented in Table II.

We see that the present method reproduces perfectly the results of the Heather-Metiu method. Moreover, the analytical asymptotic propagation during the laser pulse reduces by a factor 12 the required computing time. (6 min vs 1 h, 15 min on an IBM RS6000 350 workstation). Actually, our method allows to use eight times fewer points for the grid and the splitting operation followed by the Fourier transform with N_k points is done only 64 times, which is negligible when compared with the total number of iterations (40 000) for the whole propagation. [The gain factor in CPU time can be estimated by considering that the complexity of the algorithm is only due to Fourier transforms and thus is proportional to $N_R \ln(N_R)$.]

Essentially, the method proposed here (as in Ref. [6]) is based on a matching procedure. Indeed, the numerical wave packet is matched with a superposition of Volkov waves which are then propagated analytically. Matching procedures always involve some errors. These errors can be checked by comparing results obtained with different values of ϵ [step (ii) of the algorithm]. Indeed, decreasing the value of ϵ increases the number of splitting operations (and then of matching procedures) during

TABLE I. Dissociation branching ratios for one-, two-, or three-photon absorptions. P_{total} is the total dissociation probability. Comparison between the present method and the method of Ref. [6].

Methods	$P_{\hbar w}$ (%)	$P_{2\hbar w}$ (%)	$P_{3\hbar w}$ (%)	P_{total}
a	47.47	45.82	6.71	0.5459×10^{-3}
b	47.50	45.82	6.67	0.5464×10^{-3}

[a]Present method.
[b]Method of Ref. [6].

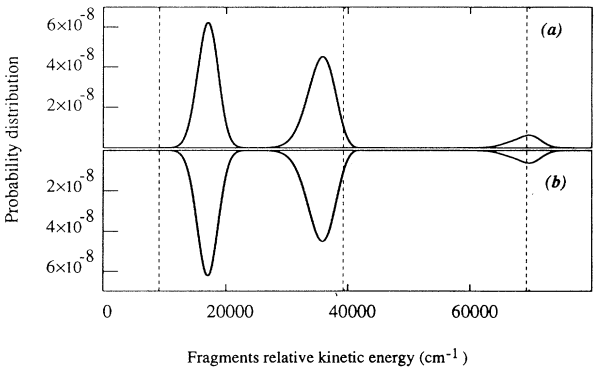

FIG. 1. Proton kinetic energy spectra with a very short laser pulse ($\tau = 5$ fs and $I = 8.7510^{13}$ W/cm^2). (a) Spectrum obtained with the present method. (b) Method of Ref. [6]. Dashed vertical lines represent energy position of one-, two-, or three-photon absorptions.

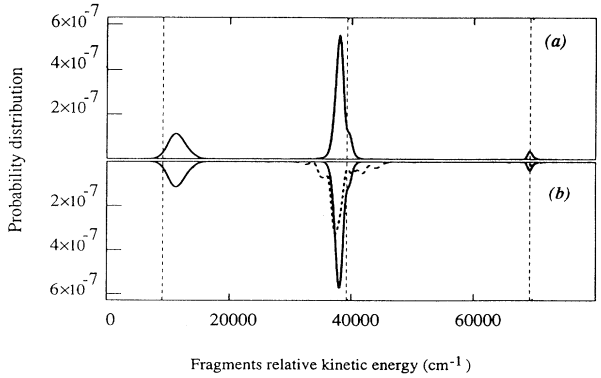

FIG. 2. Proton kinetic energy spectra with a longer laser pulse ($\tau = 20$ fs and $I = 8.75 \times 10^{13}$ W/cm^2). (a) Spectrum obtained with the present method. (b) The full line is obtained by applying the method of Ref. [6] only after the laser pulse interaction has ended. The dashed line is calculated with the same method but during the laser field interaction. Dashed vertical lines represent energy position of one-, two-, or three-photon absorptions.

TABLE II. Dissociation branching ratios for one-, two-, or three-photon absorptions. P_{total} is the total dissociation probability. Comparison between the present method and the method of Ref. [6].

Methods	$P_{\hbar\omega}$ (%)	$P_{2\hbar\omega}$ (%)	$P_{3\hbar\omega}$ (%)	P_{total}
a	26.9	70.4	2.63	0.148×10^{-2}
b	26.8	70.5	2.68	0.149×10^{-2}
c	28.7	69.4	1.89	0.140×10^{-2}

[a]Present method.
[b]Method of Ref. [6] after the end of the laser pulse.
[c]Method of Ref. [6] during the laser pulse.

the propagation. Two calculations have been made, one with $\epsilon = 10^{-9}$ which includes 52 splitting processes, and a second one with $\epsilon = 10^{-13}$ which corresponds to 1700 splittings of the wave packets. The two kinetic energy spectra are almost the same except for very small discrepancies and the maximum relative error obtained on the branching ratios is of 5%.

In Table II we have also collected the results corresponding to a calculation done with the method of Ref. [6] but without waiting for the end of the laser pulse and using the same grid as the one used for our method. Significant discrepancies are obtained. The deviation from the correct calculation is clear in Fig. 2 where the corresponding kinetic energy spectra are presented (dashed line). The wings appearing in the two-photon peaks correspond to molecules dissociating in the excited electronic state $^2\Sigma_u$, which is not the expected result; this anomaly is due to the incorrect asymptotic propagation which does not take into account the mixing of the two electronic states during the laser pulse duration. Moreover, the shape of the fragment kinetic energy spectra is very dependent upon the number of splitting operations performed during the propagation. This demonstrates that it is necessary to take into account the correct asymptotic behavior (Volkov wave), during the laser pulse, to obtain correct results.

As a second test we will compare our calculations with those of Ref. [19]. In this paper the authors calculate the fragment kinetic energy spectra resulting from the photodissociation of the H_2^+ molecule for several field intensities. The methods used consist of calculating an

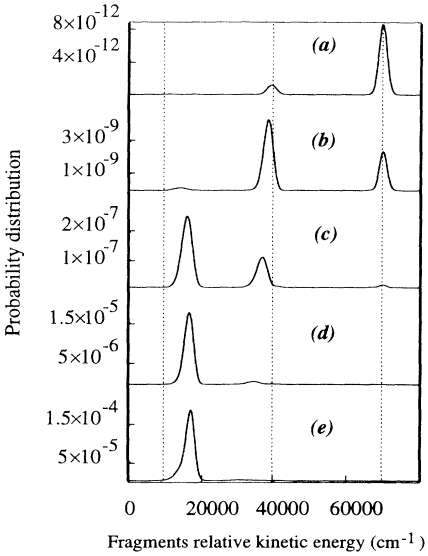

FIG. 3. Proton kinetic energy spectrum with varying intensity. The intensities are (a) $I = 3.5 \times 10^{12}$ W/cm^2, (b) $I = 3.15 \times 10^{13}$ W/cm^2, (c) $I = 8.75 \times 10^{13}$ W/cm^2, (d) $I = 1.71 \times 10^{14}$ W/cm^2, (e) $I = 3.5 \times 10^{14}$ W/cm^2. Dashed vertical lines represent energy position of one-, two-, or three-photon absorptions.

energy resolved flux and of absorbing the asymptotic part of the wave packets with the help of an optical potential. Figure 3 shows our results for the kinetic energy spectrum for five different intensities (from 3.5×10^{12} to 3.5×10^{14} W/cm^2); the pulse duration and the wavelength are the same as in Ref. [19] ($\tau = 8.6$ fs and $\lambda = 329.7$ nm). The transformation of the spectrum with the laser intensity is the same as the one presented in Ref. [19], changing from a predominant three-photon spectrum at low intensity to a one-photon peak at high intensity and passing by a two-photon dominant peak at intermediate intensity. Peak positions and widths are also very well reproduced. The evolution of the width of the peaks as the laser intensity increases and as the pulse duration changes has been recently discussed in Ref. [29]. Another striking feature appears, if we compare the spectrum of Fig. 1 with the one of Fig. 3 corresponding to the same intensity ($I = 8.75 \times 10^{13}$ W/cm^2). Not only

TABLE III. Dissociation branching ratios for one-, two-, or three-photon absorptions for varying intensities. P_{total} is the total dissociation probability.

I (TW/cm^2)	$P_{\hbar\omega}$ (%)		$P_{2\hbar\omega}$ (%)		$P_{3\hbar\omega}$ (%)		P_{total}	
	a	b	a	b	a	b	a	b
3.5	0.42	0.19	13.1	12.7	86.4	87.0	0.28×10^{-7}	0.39×10^{-7}
31.5	3.0	2.9	66.9	68.6	30.0	28.7	0.213×10^{-4}	0.296×10^{-4}
87.5	68.2	69.2	29.8	29.2	1.9	1.6	0.137×10^{-2}	0.195×10^{-2}
171.5	94.8	94.7	5.1	5.2	0.05	0.04	0.593×10^{-1}	0.797×10^{-1}
350	97.2	95.9	2.7	4.1	9×10^{-4}	7×10^{-4}	0.669×10^{-1}	0.739×10^{-1}

[a]Present method.
[b]From Ref. [19].

the widths of the peaks are different but also their positions. Indeed, we can see that the one-photon peak is shifted to higher energy by $\simeq 7400$ cm^{-1} and the two-photon peak is shifted to lower energy by $\simeq 2400$ cm^{-1}, when the pulse duration decreases from $\tau = 100$ fs to $\tau = 8.6$ fs. These shifts which may be related to the uncertainty principle ($\tau = 8.6$ fs corresponds to an energy width of $\simeq 7700$ cm^{-1}) are not yet well understood and will be the subject of a forthcoming paper. The branching ratios for peaks corresponding to one-, two-, and three-photon transitions and the total photodissociation probability for several field intensities calculated with the two methods are collected in Table III.

The deviations observed in the total photodissociation probability may come from the different transition dipole moments taken in this work, indeed, we must take a transition dipole moment which has a correct asymptotic behavior. The different momentum space resolutions used in the two calculations (512 points in Ref. [19] and 2048 points here) may be the origin of the small disagreements obtained in the branching ratios. It is important to note that not only the fragment analysis methods but also the propagation methods are different in the two calculations. The general good agreement obtained between the two methods (the absolute error is of the order of 1%; this implies that the relative error on small numerical values may be large) demonstrates the validity of our asymptotic fragment analysis but also shows the consistency of the two different propagation schemes.

IV. CONCLUSION

We have presented an efficient method to solve the problem of intense field photodissociation of homonuclear ions, which possess an electronic transition moment diverging with the internuclear separation. The method is a generalization of the scheme developed by Heather and Metiu [6] for finite range interaction molecular systems. It is clear that this method can be applied to any photofragmentation which presents an asymptotic coupling or interaction varying linearly with the interfragment separation. For instance, the calculation of the electron kinetic energy spectrum, resulting from the photoionization of an atom by an intense laser field, may be done with the same type of method.

The analytical propagation to infinite time of the asymptotic wave packet's parts allows a description of the full wave packets and restricts the numerical effort to the propagation in a previously fixed region of space, regardless of the laser pulse duration. The method has been successfully tested by calculating the fragment kinetic energy distribution resulting from the photodissociation of the H_2^+ molecule. Good agreement has been found with already published results [19]. By comparison with the efficient method of Ref. [6], it has been shown that our method reduces by a factor 12 the required computing time. Recently many experimental and theoretical studies have focused on the rotational motion of the molecule during the photodissociation. The inclusion of this additional degree of freedom requires heavy numerical calculations. The extension of the method presented here, to take into account the rotation of the molecule and therefore for calculating energy resolved fragment angular distribution, is in progress and will be the subject of a future work.

ACKNOWLEDGMENTS

I thank Professor O. Atabek for suggesting this work to me. I would like to thank Professor N. Moiseyev for many valuable discussions. A grant of computing time from the Institut du Diveloppement et des Resources en Informatique Scientifique (IDRIS) is also gratefully acknowledged.

[1] U. Peskin, O. E. Alon, and N. Moiseyev, J. Chem. Phys. **100**, 7310 (1994).
[2] E. J. Heller, J. Chem. Phys. **62**, 1544 (1975).
[3] G. G. Balint-Kurti, R. N. Dixon, and C. C. Martson, J. Chem. Soc. Faraday Trans. **86**, 1741 (1990).
[4] C. Leforestier, Chem. Phys. **87**, 241 (1984).
[5] R. N. Dixon, C.C Marston, and G. G. Balint-Kurti, J. Chem. Phys. **93**, 6520 (1990).
[6] R. Heather and H. Metiu, J. Chem. Phys. **86**, 5009 (1987).
[7] R. S. Mulliken, J. Chem. Phys. **7**, 20 (1939).
[8] D. E. Ramaker and J. M. Peek, At. Data **5**, 167 (1973).
[9] M. Y. Ivanov and P. B. Corkum, Phys. Rev. A **48**, 580 (1993).
[10] M. Chrysos, O. Atabek, and R. Lefebvre, Phys. Rev. A **48**, 3845 (1993).
[11] M. Chrysos, O. Atabek, and R. Lefebvre, Phys. Rev. A **48**, 3855 (1993).
[12] E. E. Aubanel, J. M. Gauthier, and A. D. Bandrauk, Phys. Rev. A **48**, 2145 (1993).
[13] E. Charon, A. Giusti-Suzor, and F. H. Mies, Phys. Rev. Lett. **71**, 692 (1993).
[14] J. Perie and G. Jolicard, J. Phys. B **26**, 4491 (1993).
[15] A. Zavriyev, P. H. Bucksbaum, H. G. Muller, and D. W. Schumacher, Phys. Rev. A **42**, 5500 (1990).
[16] A. Zavriyev, P. H. Bucksbaum, B. Yang, and L. F. Dimauro, Phys. Rev. A **44**, R1458 (1991).
[17] A. Giusti-Suzor, X. He, O. Atabek, and F. H. Mies, Phys. Rev. Lett. **64**, 515 (1990).
[18] A. Bandrauk and H. Shen, Chem. Phys. Lett. **176**, 428 (1991).
[19] G. Jolicard and O. Atabek, Phys. Rev. A **46**, 5845 (1992).
[20] L. V. Keldysh, Zh. Eksp. Teor. Fiz. **47**, 1945 (1964) [Sov. Phys. JETP **20**, 1307 (1965)].
[21] H. R. Reiss, Phys. Rev. A **22**, 1786 (1980).
[22] H. D. Feit, J. A. Fleck, and A. Steiger, J. Comput. Phys. **47**, 412 (1982).
[23] D. Kosloff and D. Kosloff, J. Comput. Phys. **52**, 35 (1983).
[24] C. E. Dateo and H. Metiu, J. Chem. Phys. **95**, 7392

(1991).
[25] H. Filon, Proc. R. Soc. Edinburgh **49A**, 39 (1928).
[26] A. Bandrauk and H. Shen, J. Chem. Phys. **99**, 1185 (1993).
[27] J. M. Peek, J. Chem. Phys. **43**, 3004 (1965).
[28] D. R. Bates, J. Chem. Phys. **19**, 1122 (1951).
[29] O. Atabek and G. Jolicard, Phys. Rev. A **49**, 1186 (1994).